Journal of Plant Pathology (2020) 102:39–46
https://doi.org/10.1007/s42161-019-00370-y

ORIGINAL ARTICLE

Antifungal activity of Carbendazim-conjugated silver nanoparticles against anthracnose disease caused by *Colletotrichum gloeosporioides* in mango

Raghavendra Shivamogga Nagaraju[1] · Raghu Holalkere Sriram[1] · Rajeshwara Achur[1]

Received: 13 November 2018 / Accepted: 22 July 2019 / Published online: 26 August 2019

Abstract
Mango is one of the popular fruits in the tropical region including India and the production of this is adversely affected by Anthracnose disease caused by *Colletotrichum gloeosporioides*. This fungal infection during pre-and post-harvesting seasons causes significant economic loss and thus there is a need for effective fungicide to control the disease. Currently, many fungicides including Carbendazim at high concentrations are being used which is a serious environmental hazard. Recently, silver nanoparticles (AgNPs) are being used as a potent means of controlling various pathogenic microorganisms. In this study, we have synthesized Carbendazim-conjugated silver nanoparticles (Cz-AgNPs) by a chemical method and tested their efficacy against *C. gloeosporioides*, *in vitro*. The Cz-AgNPs were characterized by UV-Visible, FTIR, SEM and XRD analysis. The shape of Cz-AgNPs was found to be spherical with an average particle size of 19–24 nm. The antifungal activity of Cz-AgNPs was found to be dose-dependent and the maximum potency was observed at a low concentration of 0.1% as compared to fungicide alone at 1% concentration. These results indicate that the Cz-AgNPs could be effectively used to control anthracnose disease in mango and in other crops as well. Further studies with other fungicides and field studies are in progress.

Keywords Anthracnose disease · *Colletotrichum gloeosporioides* · Carbendazim · Silver nanoparticles

Introduction

Agricultural production has reduced worldwide over the past few years due to plant diseases. Millions of dollars have been invested in efforts to manage these plant diseases. Various natural and artificial methods including pesticide are employed for the control of these diseases. In recent years, environmental and health hazards caused by excessive use of pesticides have been widely discussed and thus there is a need for reducing the use of pesticides for the control of plant pathogens. A promising alternative in this direction is the use of silver nanoparticles as antimicrobial agents and the recent technological advances are even making their production more economical (Jo et al. 2009). Thus, there is a need for extensive research on fungicide conjugated silver nanoparticles which minimizes the use of fungicide while enhancing the antifungal potency of silver nanoparticles.

Mango (*Mangifera indica* L.) is considered as one of the most popular fruits in the tropical area and increasingly so in many countries including India. Mango fruits are very sensitive and subjected to decay under extreme environmental conditions including temperature and general fruit freshness is limited due to the rapid ripening, storage, handling and transportation damages. In addition to these limitations, Anthracnose disease caused by *Colletotrichum gloeosporioides* is the major postharvest disease of mango in all mango producing areas of the world (Dodd et al. 1989; Swart et al. 2002). The disease occurs as quiescent infections on immature fruit and the caused damage is more important in the postharvest period (Muirhead and Gratitude 1986; Dodd et al. 1997). Fungicides, either as preharvest or postharvest treatments, form the main approach to reduce losses from anthracnose.

Anthracnose disease was first identified in Chilly plant in 1890 (New Jersey, USA) by Halsted. The word 'Anthracnose' is derived from a Greek word meaning 'coal', which is the common name for plant disease characterized by very dark, sunken lesions, containing spores (Fig. 1). Generally,

✉ Raghu Holalkere Sriram
hsr1983@gmail.com

[1] Department of Biochemistry, Kuvempu University, Shankarghatta, Karnataka 577451, India

Fig. 1 Anthracnose disease symptoms in mango

anthracnose disease is caused by *Colletotrichum* species which belongs to the Kingdom Fungi; Phylum Ascomycota, Class Sordariomycetes; Order Phyllachorales and Family Phyllachoraceae.

Carbendazim is a widely used, broad-spectrum benzimidazole fungicide and a metabolite of benomyl. The other names of Carbendazim are Mercarzole and Carbendazole. It is also employed as a casting worm control agent in amenity turf situations such as golf greens, tennis courts etc. This fungicide is used to control plant diseases in cereals and fruits, including citrus, bananas, mango, strawberries, pineapples, and pomes. The IUPAC name is Methyl *1H*-benzimidazol-2-ylcarbamate and the molecular formula is $C_9H_9N_3O_2$. The structure of Carbendazim is as shown in Fig. 2.

The term "nano" is originated from Greek language meaning extremely small and the nanoparticles are between 1 and 100 nm in size (Rai et al. 2008). The nanoparticles can be synthesized by three different approaches including physical, chemical, and biological methods. Among the various type of nanoparticles, the silver nanoparticles (AgNPs) are known to exhibit broad spectrum of bactericidal and fungicidal activities (Ahamed et al. 2010). This property has made them as

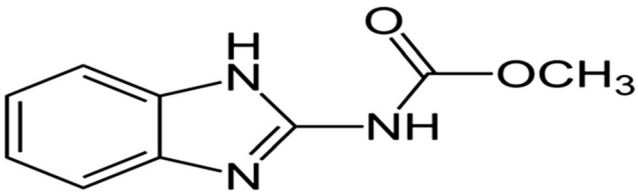

Fig. 2 Structure of Carbendazim

extremely popular in a diverse range of consumer products, textile industry, and environmental treatments such as air and water disinfection. Silver is generally used in nitrate form to induce antimicrobial effect, but when silver nanoparticles are used, the activity is enhanced due to increase in the surface area. One of the recent potential applications of silver nanoparticles is in the management of plant diseases. Silver displays multiple modes of inhibitory action against microorganisms and therefore, it may be relatively safe for control of various plant pathogens, compared to synthetic fungicides (Park et al. 2006, Eckert 1990 and 1991).

Material and methods

Synthesis of silver nanoparticles using sodium borohydride as a reducing agent

Silver nanoparticles (AgNPs) were synthesized through the reduction of silver nitrate ($AgNO_3$) by sodium borohydride ($NaBH_4$). Double distilled deionized water was used to prepare both the reagents ($AgNO_3$ and $NaBH_4$). Different volumes (5, 10, 15 ml of 0.001 M) of silver nitrate were added drop wise to 30 ml of 0.1% pre chilled sodium borohydride. The reaction mixture was stirred vigorously on a magnetic stirrer for about 5 to 10 min. The solution turned to light yellow after the addition of 10 ml of silver nitrate and to brighter yellow when all of the silver nitrate had been added. The stirring was continued even after all the silver nitrate was added, which turned the solution darker yellow first, then violet and finally grayish in colour. Finally, the colloid breaks down to settle out the particles.

$$AgNO_3 + NaBH_4 \rightarrow Ag + 1/2\ H_2 + 1/2B_2H_6 + NaNO_3$$

Synthesis of Carbendazim conjugated silver nanoparticles (Cz-AgNPs)

The fungicide, Carbendazim (0.1%) was mixed with 1% sodium borohydride, this mixture was pre chilled for 15 min. Silver nitrate (0.001 M) solution was added drop wise to this mixture with vigorous stirring on a magnetic stirrer for about 5 to 10 min. The solution turned to dark yellow after the addition of 15 ml of silver nitrate.

UV-visible spectroscopy

The optical properties of synthesized silver nanoparticles were determined by using UV-Visible spectrometry. The UV-Visible absorption spectra of AgNPs and Cz-AgNPs were observed in the range 350 nm to 450 nm.

Scanning electron microscopy (SEM) analysis

The SEM analysis is the best method for determining the surface topography and 3D view of the synthesized nanoparticles. The morphological characteristics of AgNPs and Cz-AgNPs was established by SEM. Thin films of the samples were prepared on a carbon coated copper grid by dropping a very small amount of the sample on the SEM grid and the film was allowed to dry by keeping it under a mercury lamp for 5 min and then subjected for SEM analysis.

X-ray diffraction analysis

The crystallite domain size was calculated from the width of XRD peaks, assuming that they are free from non-uniform strains, using the Scherrer formula.

$$D = 0.94\,\lambda/\beta\,\mathrm{Cos}\,\theta$$

where D is the average crystallite domain size perpendicular to the reflecting planes, λ is the X-ray wavelength, β is the full width at half maximum (FWHM), and θ is the diffraction angle. To eliminate additional instrumental broadening the FWHM was corrected, using the FWHM from a large grained Si sample. β corrected = $(FWHM^2sample\text{-}FWHM^2si)^{1/2}$.

The lyophilized AgNPs and Cz-AgNPs were coated on the grid and subjected to X-ray diffraction (XRD) measurements. The analysis was carried out using X-ray diffractometer with an operating voltage of 45KV and a current of 0.8 mA (Unisantis XMD-300, Swiss). The diffraction patterns were recorded by Cu-Kα radiation of wavelength 1.54 A° in the region of 2θ from 0° to 60°.

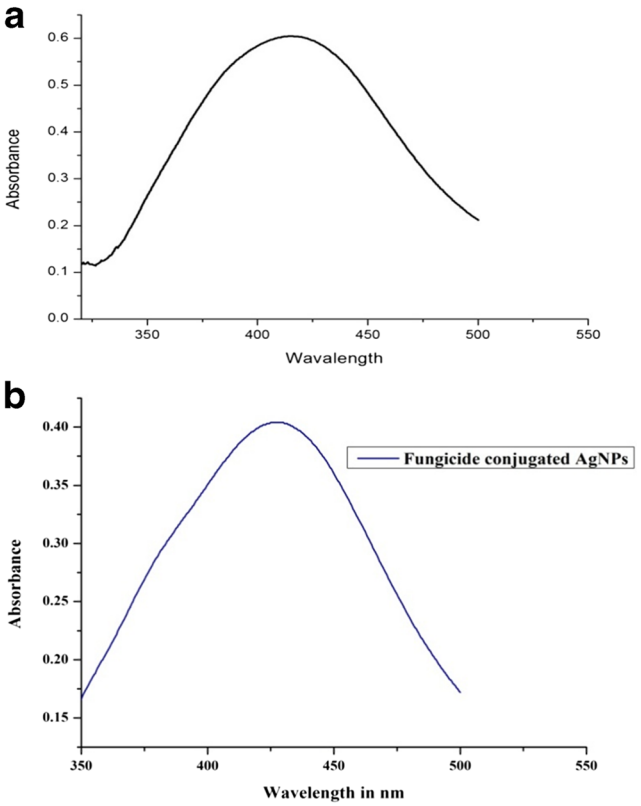

Fig. 4 **a** UV-Vis absorption spectra of silver nanoparticles prepared using chemical method. **b** UV-Vis absorption spectra of conjugated silver nanoparticles prepared using chemical method

Fourier transform infrared spectroscopy

The AgNPs, Carbendazim and Cz-AgNPs were subjected to Fourier transform infrared (FT-IR) spectroscopy (Bruker, USA) in order to analyze their spectra. The analysis was carried out with potassium bromide (KBr) pellets, recorded in the range 500–4000 cm^{-1}.

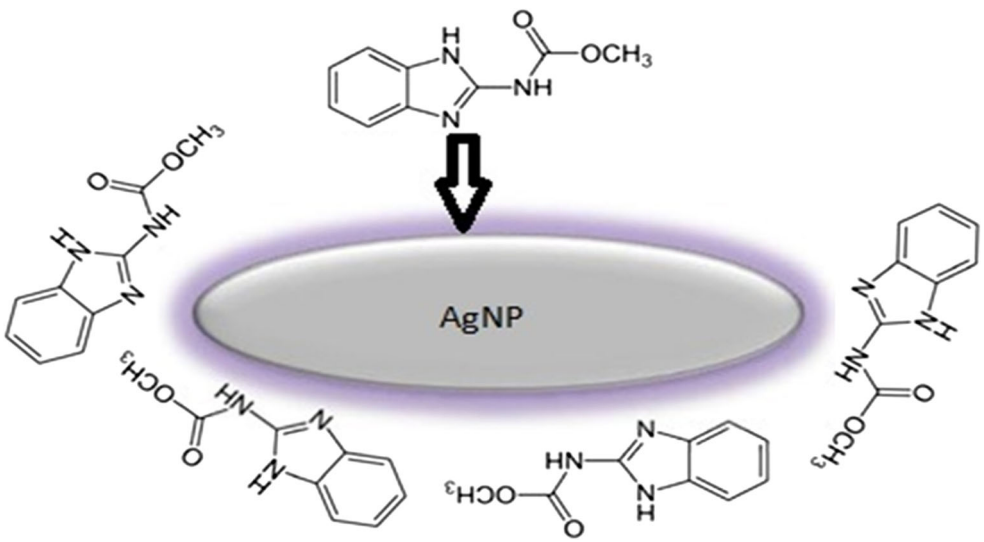

Fig. 3 Schematic representation of Carbendazim and its surface adsorption on the silver nanoparticles (Ag NPs)

In vitro antifungal activity of AgNPs and Cz-AgNPs

The antifungal activity of AgNPs and Cz-AgNPs was investigated by well plate method, in vitro. Different volumes (25 μl, 50 μl, 75 μl and 100 μl) of the synthesized AgNPs and Cz-AgNPs were added to wells made in the solidified potato dextrose agar media. The plates were incubated at 35 °C for 48–72 h for the visualization of inhibition zones. The inhibition of control (1% Carbendazim alone) was also examined along with NPs.

Results and discussion

Characterization of AgNPs and Cz-AgNPs

The addition of Carbendazim during the chemical synthesis of AgNPs results in the adsorption on to the surface of AgNPs. This can be attributed to weak electrostatic interaction between N-atom of Carbendazim and Ag atom in AgNPs (Fig.3).

UV-visible spectroscopy

The UV-Visible spectroscopy is one of the most widely used techniques for the structural characterization of AgNPs. The absorption band in 350 to 550 nm region is typical for the AgNPs (Kadir et al. 2005). The UV-visible spectra showed absorption bands in 350 to 550 nm region which confirms the formation of AgNPs (Sastry et al. 1997; Henglein 1993; Sastry et al. 1998). In this study, we found that the AgNPs and Cz-AgNPs showed the characteristic absorption peak at 412 nm and 426 nm, respectively (Fig. 4a and b).

Scanning electron microscopy (SEM) analysis

Microscopic surface features including morphology and particle size of synthesized AgNPs and Cz-AgNPs were assessed by SEM analysis. The nanoparticles were found to be spherical in shape with a diameter ranging from 19 to 24 nm and 22 to 26 nm respectively. SEM image also confirms that the synthesized nanoparticles are well separated with no aggregation (Fig. 5a and b).

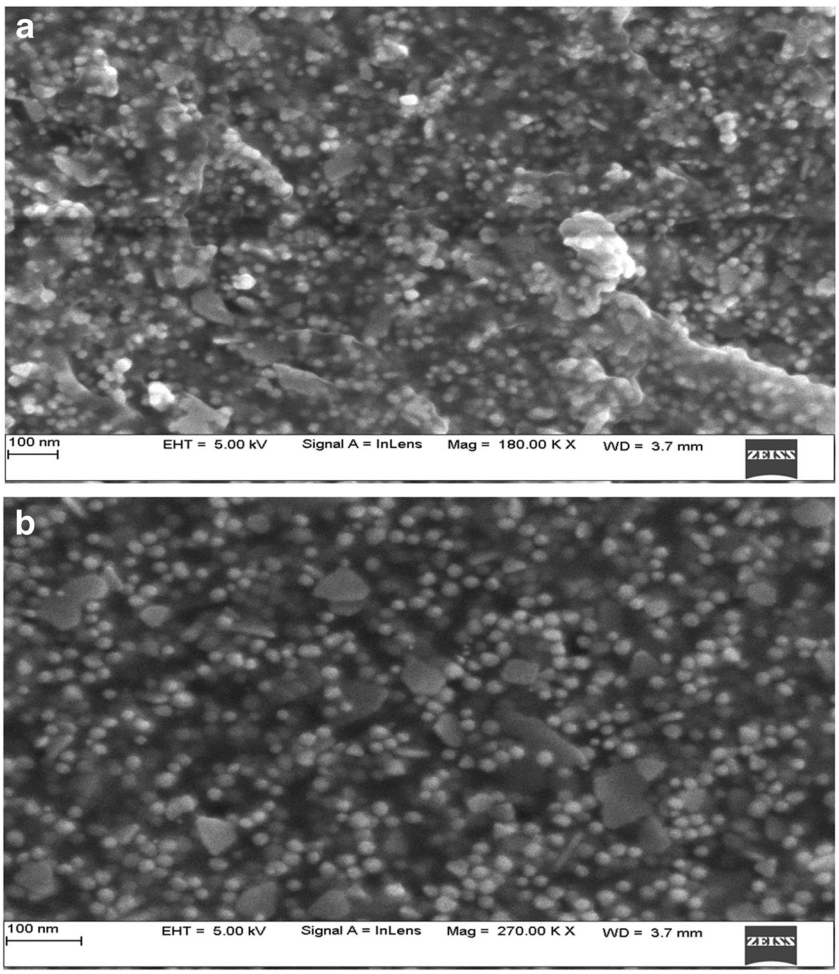

Fig. 5 **a** SEM images of silver nanoparticles. **b** SEM images of fungicide conjugated silver nanoparticles

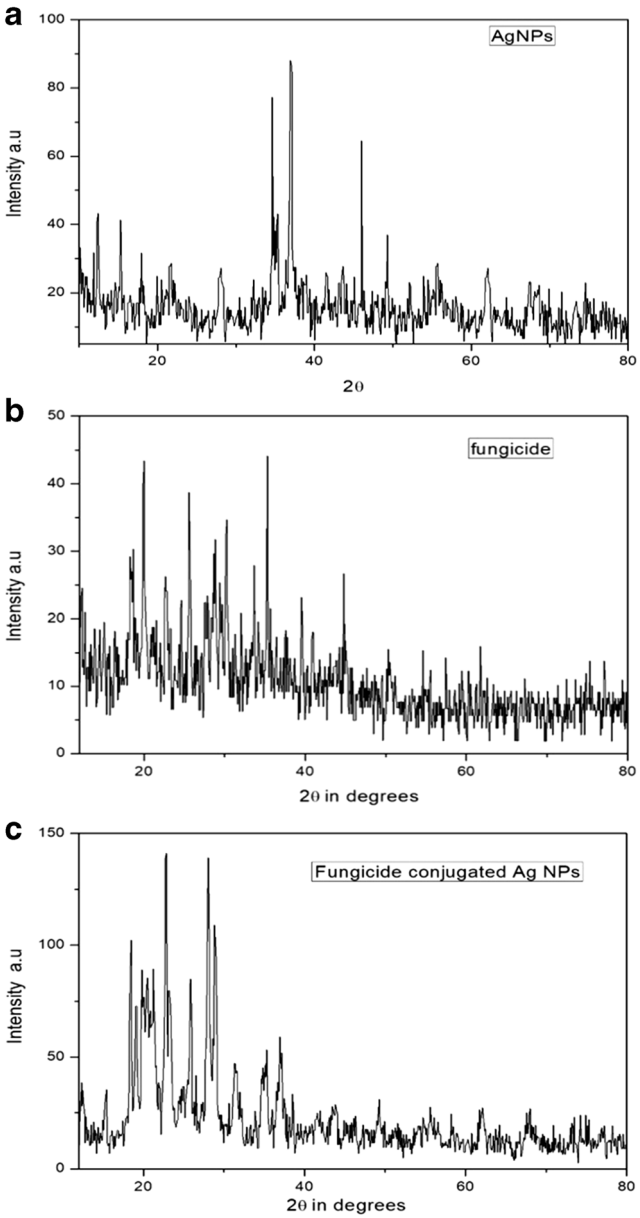

Fig. 6 **a** XRD pattern of AgNPs. **b** XRD pattern of the fungicide Carbendazim. **c** XRD pattern of fungicide conjugated AgNPs

X-ray diffraction analysis

The synthesized AgNPs and Cz-AgNPs were subjected to X-Ray diffraction studies, to understand the crystallinity and to establish the average particle size. As shown in Fig. 6a, the XRD pattern of AgNPs has prominent diffraction peaks of the 2θ values of 36.97°, 46.02°, 62.10° and 74.47° which can be assigned to (111), (200), (220) and (311) planes, respectively, with some minor peaks (Liang et al. 2010).

The XRD pattern of Carbendazim alone showed prominent characteristic peaks of 2θ at 19.83°, 25.54° and 35.25° (Fig. 6b) which confirms the presence of Carbendazim (Yunlong et al. 2009). The XRD pattern of Cz-AgNPs showed characteristic peaks of 2θ at 18.36°, 25.81°and 34.58° corresponding to Carbendazim and the peaks of 2θ at 36.84°, 49.21° 61.97° and 74.60° corresponding to AgNPs (Fig. 6c). The data confirm that Carbendazim has been successfully adsorbed on the surface of AgNPs.

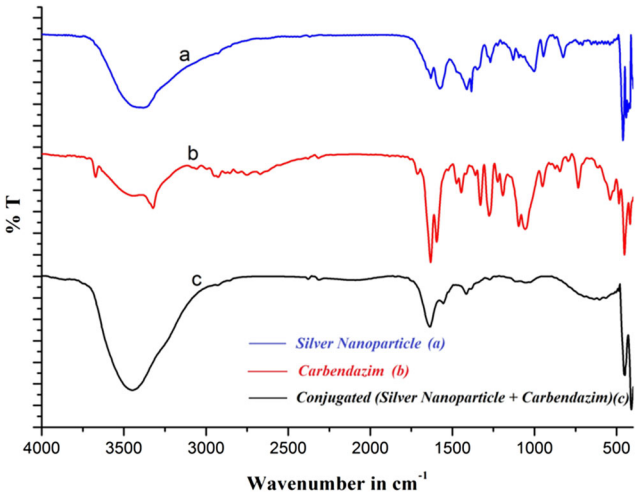

Fig. 7 Fourier transform infrared spectroscopy of **a** AgNPs **b** Fungicide Carbendazim and, **c** Conjugated (AgNPs + Carbendazim). [N-H bond – 3500-3300 nm, C=N bond —1650-1550 nm]

Fourier transform infrared spectroscopy

The FTIR spectra of synthesized AgNPs showed various absorption bands for different chemical groups (Fig. 7). The broad band at 3384.49 cm^{-1} showed the stretching vibrations of –N-H and –O-H groups, the absorption bands at 1630.78, 1384.50, and 1002.23 cm^{-1} corresponds to –C=O, –C=C–, and –C-O groups, respectively. Additionally, the presence of absorption band at

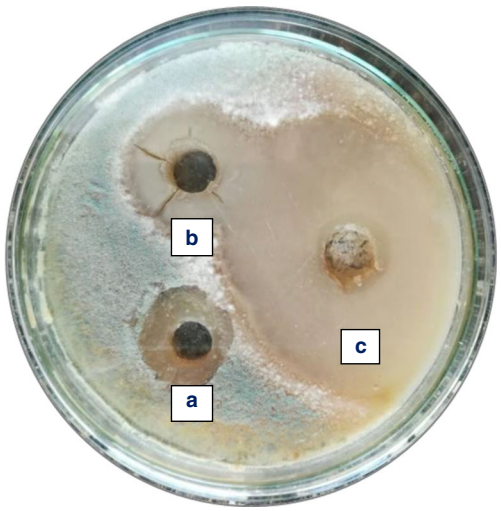

Fig. 8 Antifungal activity of **a** AgNPs, **b** Fungicide and **c** fungicide conjugated AgNPs by disc diffusion method

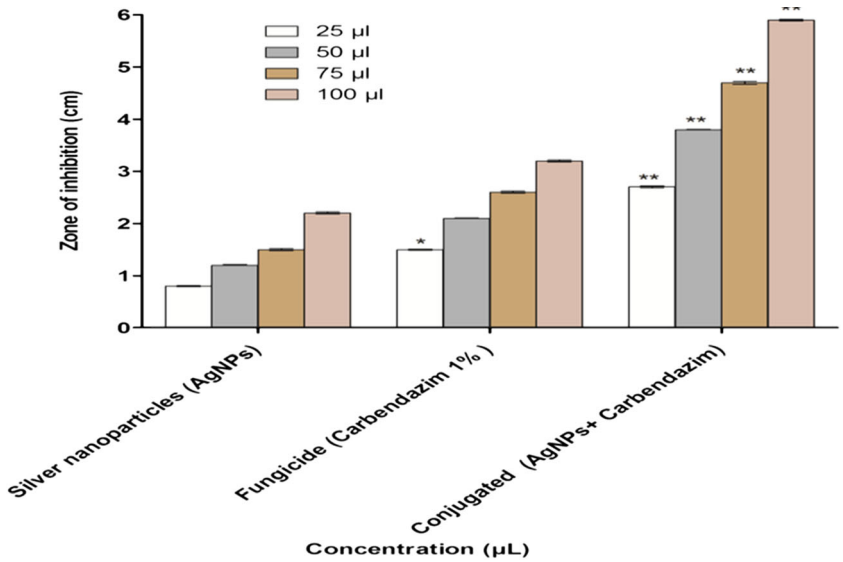

Fig. 9 Inhibition zone of AgNPs, Carbendazim and Cz-AgNPs

1129.74 cm^{-1} confirms the presence of –C-N group (Bahrami-Teimoori et al. 2017).

The FTIR spectrum of Carbendazim shows characteristic peaks at 3323.58, 1632.19, 1595.23 and 1096.54 cm^{-1} which confirms the presence of Carbendazim as shown earlier (Chan et al. 2015). The FTIR spectrum of Cz-AgNPs shows distinct peaks at 3449.83 cm^{-1} illustrating the stretching vibrations confirming the AgNPs. The peaks at 1636.86 and 1555.43 cm^{-1} establish the adhesion of Carbendazim on the AgNPs.

Antifungal activity of AgNPs and Cz-AgNPs

The antifungal potential of AgNPs and Cz-AgNPs was assessed against *Colletotrichum gloeosporioides* which is known to cause anthracnose disease in mangoes. The results showed that the inhibition of fungal growth was observed with both AgNPs as well as Cz-AgNPs (Figs. 8 and 9). Carbendazim (1%) significantly inhibited with an inhibition zone of diameter 3.2 cm which is 45% more than the AgNPs which showed the inhibition zone of diameter 2.2 cm. Further, the fungicide conjugated AgNPs exhibited highest growth inhibition of *Colletotrichum gloeosporioides* (~168%) as compared to fungicide Carbendazim alone with an inhibition zone of 5.9 cm. The inhibition of growth was also found to be dose-dependent with respect to the concentration of Cz-AgNPs (Table 1). The comparison of inhibition data shows the high significance when compared between Cz-AgNPs and AgNPs ($p < 0.002$), and Carbendazim ($p < 0.005$).

Previously various volatile plant essential oils were tested against Anthracnose disease in pepper fruit (Hong et al. 2015). Plant extracts along with chitosan have also been tested on anthracnose disease in papaya fruit (Bautista-Banos et al. 2003). This is the first instance where we are reporting the conjugation of silver nanoparticle with the pesticide Carbendazim. The results illustrate the synergistic effect of silver nanoparticles conjugated with pesticide Carbendazim.

Conclusions

Currently there are many chemical fungicides to control plant pathogens which are being used at very high concentrations thus causing environmental pollution. Thus, there is a great need to reduce the use of high concentration of these fungicides to control plant pathogens which affect several commercial crops worldwide. It has been very well established that

Table 1 The effect of AgNPs and Cz-AgNPs on the growth inhibition of *Colletotrichum gloeosporioides*

	Zone of inhibition (cm)#			
	25 µl	50 µl	75 µl	100 µl
Silver nanoparticles (AgNPs)	0.8 ± 0.01	1.2 ± 0.02	1.5 ± 0.02	2.2 ± 0.02
Fungicide (Carbendazim 1%)	1.5 ± 0.01*	2.1 ± 0.01	2.6 ± 0.02	3.2 ± 0.02
Conjugated (AgNPs+ Carbendazim)	2.7 ± 0.02**	3.8 ± 0.01**	4.7 ± 0.03**	5.9 ± 0.02**

#Values represent the mean (± SE) from three experiments, ($n = 4$)

*The values of Cz-AgNPs were significant compared with Carbendazim ($p < 0.005$)

**The values Cz-AgNPs were significant compared with the AgNPs ($p < 0.002$)

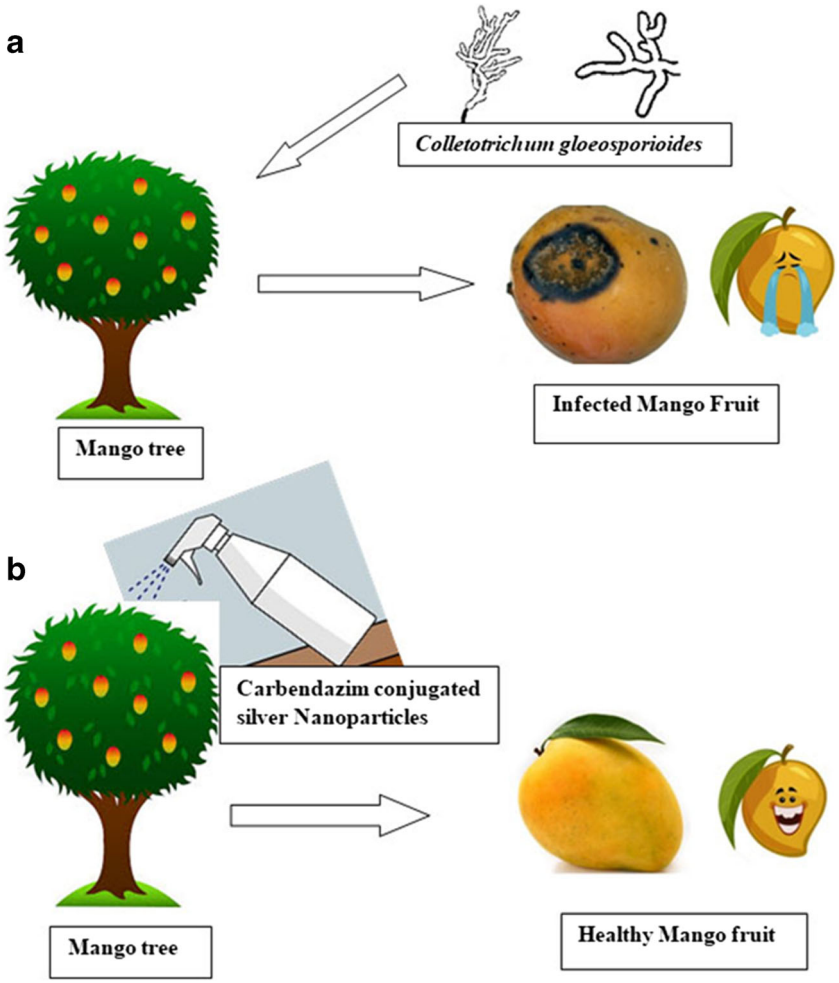

Fig. 10 Schematic Diagram of **a** *Colletotrichum gloeosporioides* infection to the mango tree **b** Application of Carbendazim conjugated silver nanoparticles which prevents the infection of *Colletotrichum gloeosporioides*

plain AgNPs alone can be an effective means of controlling plant pathogens. However, in the present study, we have used Cz-AgNPs as an economical and environmental friendly method to control *C. gloeosporioides* which causes anthracnose disease in mango (Fig. 10).

The synthesized AgNPs and Cz-AgNPs were characterized by UV-Vis spectra, SEM, XRD and FT-IR analysis. The adsorption of the fungicide Carbendazim onto AgNPs were confirmed by the FT-IR spectra and further evidenced by the characteristic XRD pattern of Cz-AgNPs as compared to AgNPs and Carbendazim. The results showed high significance of the inhibition by Cz-AgNPs when compared with AgNPs at a concentration of 100μL ($p < 0.002$) when compared with Carbendazim alone. The data clearly indicates that the AgNPs conjugated with Carbendazim greatly enhances the antifungal potency of the fungicide. Moreover, the lower concentration of fungicide makes it environmental friendly when conjugated to AgNPs. These results clearly demonstrate the utility of Cz-AgNPs in enhancing the antifungal potency of both Carbendazim as well as AgNPs. These Cz-AgNPs could potentially be used in the field to control anthracnose disease caused by *C. gloeosporioides* in mango and other crops as well.

Compliance with ethical standards

Conflict of interest The authors declare that they have no conflict of interest.

Ethical approval "This article does not contain any studies with human participants or animals performed by any of the authors."

Informed consent Not applicable.

References

Ahamed M, Alsalhi MS, Siddiqui MK (2010) Silver nanoparticle applications and human health. Clin Chim Acta 411:1841–1848

Bahrami-Teimoori B, Nikparast Y, Hojatianfar M, Akhlaghi M, Ghorbani R, Pourianfar HR (2017) Characterization and antifungal activity of silver nanoparticles biologically synthesised by *Amaranthus retroflexus* leaf extract. J Exp Nanosci 12:129–139

Bautista-Banos S, Hernandez-Lopez M, Bosquez-Molina E, Wilson CL (2003) Effect of chitosan and plant extracts on growth of *colletotrichum gloeosporioides*, anthracnose levels and quality of papaya fruit. Crop Prot 22:1087–1092

Chan b, Sufen Z, Lei H, Ye Q (2015) Starch-based hydrogel loading with Carbendazim for controlled-release and water absorption. Carbohydr Polym 125:376–383

Dodd JC, Jeffries P, Jeger MJ (1989) Management strategies to control latent infection in tropical fruits. Asp Appl Biol 20:49–56

Dodd JC, Prusky D, Jeffries P (1997) Fruit diseases. In: Litz RE (ed) The mango: botany, production and uses. CAB, International, UK, pp 257–280

Eckert JW (1990) Recent development in the chemical control of post-harvest diseases. In: R.E.Paull (ed.) Tropical Fruit in International Trade. Acta Hortic 269:477–494

Eckert JW (1991) Role of chemical fungicides and biological agents in post harvest disease control. Biological control of postharvest diseases of fruits and vegetable s. In: Workshop proceedings, vol. 92, Shepherdstown, VA, September., 1990. US Department of Agriculture, Agricultural Research Service Publications, 14–30

Henglein A (1993) Physicochemical properties of small metal particles in solution: 'microelectrode' reactions, chemisorption, composite metal nanoparticles, and the atom-to- metal transition. Phys Chem B 97: 5457–5471

Hong JK, Yang HJ, Jung H, Yoon DJ, Sang MK, Jeun Y-C (2015) Application of volatile antifungal plant essential oils for controlling pepper fruit anthracnose by *colletotrichum gloeosporioides*. Plant Pathol J 31(3):269–277

Jo YK, Kim BH, Jung G (2009) Antifungal activity of silver ions and nanoparticles on hytopathogenic fungi. Plant Dis 93:1037–1043

Kadir A, Lakowiez JR, Geddes CD (2005) Rapid deposition of triangular silver nanoparticles on planar surfaces: application to metal-enhanced fluorescence. J Phys Chem B 109:6247–6251

Liang FH, Yong GX, Yuan ZZ, Min MA (2010) Study on the crystalline structure and thermal stability of silver oxide films deposited by direct-current reactive magnetron sputtering methods. J Korean Phys Soc 56:1176–1179

Muirhead IF, Gratitude R (1986) Mango diseases. In: Proceedings of the First Australian mango research workshop, Cairns, November 26–30. Commonwealth Scientific and Industrial Research Organisation (CSIRO), 248–252

Park HJ, Kim SH, Kim HJ, Choi SH (2006) A new composition of nanosized silica-silver for control of various plant diseases. Plant Pathol J 22:295–302

Rai M, Yadav A, Gade A (2008) CRC 675-current trends in phytosynthesis of metal nanoparticles. Crit Rev Biotechnol 28: 277–284

Sastry M, Mayya KS, Bandyopadhyay K (1997) pH dependent changes in the optical properties of carboxylic acid derivatized silver colloidal particles. Colloids Surf A Physicochem Eng Asp 127:221–228

Sastry M, Patil V, Sainkar SR (1998) Electrostatically controlled diffusion of carboxylic acid derivatized silver colloidal particles in thermally evaporated fatty amine films. Phys Chem B 102:1404–1410

Swart SH, Serfontein JJ, Kalinowski J (2002) Chemical control of post-harvest diseases of mango—the effect of Prochloraz, thiabendazole and fludioxonil on soft brown rot, stem-end rot and anthracnose. S.a. Mango growers' Assoc. Res J 22:55–62

Yunlong YU, Xiaoqiang G, Yueqin H (2009) Effects of repeated applications of fungicide carbendazim on its persistence and microbial community in soil. J Environ Sci 21:179–185